Theoretical investigation on forbidden transition properties of fine-structure splitting in ^{2}D state for K-like ions with $26 \leqslant Z \leqslant 36$*

Jian-Peng Liu(刘建鹏)[1], Cheng-Bin Li(李承斌)[2,†], and Hong-Xin Zou(邹宏新)[1,‡]

[1] *Interdisciplinary Center of Quantum Information, National University of Defense Technology, Changsha* 410073, *China*

[2] *State Key Laboratory of Magnetic Resonance and Atomic and Molecular Physics, Wuhan Institute of Physics and Mathematics, Chinese Academy of Sciences, Wuhan* 430071, *China*

(Received 24 March 2017; revised manuscript received 20 June 2017; published online 20 August 2017)

Excitation energies, magnetic dipole, and electric quadrupole transition probabilities of the 3d $^2D_{3/2}$–3d $^2D_{5/2}$ transition in the potassium-like (K-like) sequence with $26 \leqslant Z \leqslant 36$ are investigated by using the multi-configuration Dirac–Hartree–Fock (MCDHF) method. The contributions of the electron correlations, Breit interaction, and the leading-order quantum electrodynamic (QED) effects on the transition properties are analyzed. The present results are interested in the laboratory tokamak and the astronomical observations. Furthermore, the feasibility of these ions for the highly charged ion (HCI) clocks is discussed. Considering the wavelength of lasers and manipulation process of the atomic clocks, Cu^{10+} and Zn^{11+} are recommended as promising candidates with achievable quality factors at the 10^{15} level.

Keywords: forbidden transition probabilities, potassium-like ions, MCDHF method

PACS: 32.70.Cs, 31.15.V–, 31.15.vj **DOI:** 10.1088/1674-1056/26/10/103201

1. Introduction

The forbidden magnetic dipole (M1) and electric quadrupole (E2) transition properties of ions are of great importance in the diagnostic processes of the plasmas, due to the fact that the increment of populations in metastable states is caused by the low rates of collisional de-excitations in the upper states of the forbidden transitions. This is vital to infer the plasma temperature and dynamics by observing the transitions between the fine-structure levels of the ground state of HCIs in the laboratory tokamak.[1,2] The intensities of the forbidden transitions are also used in the identification of the observed spectra, which are important to acquire the abundances of the atomic elements in astronomical objects.[3,4] Since the spectral range is wide, the accurate calculations of the atomic parameters along the isoelectronic sequences are imperative. On the other hand, the HCIs are proposed as the candidates for making new high-precision atomic clocks with accuracy below 10^{-19}, which will be useful in the applications on the time service, navigation, communication, fundamental physics, and so forth.[5–9] The breakthrough of the cooling and trapping techniques for the HCIs has shed light on the realization of the new ultra-precise optical frequency standards.[10] However, finding a suitable ion is still under investigation, which is compatible with the experimental feasibility, simplicity, and high index.[11]

With the development of the theoretical methods in atomic physics and the capacity of the available computers, the transition properties in different isoelectronic sequences have been widely studied for the astrophysical and laboratory interests in recent years (see Refs. [12]– [18] and the references therein). For the K-like ions, Biémont *et al.* have calculated the energy levels and transition properties of the 3d configuration with $22 \leqslant Z \leqslant 47$.[19] Similarly, Ali *et al.* have presented their results with $19 \leqslant Z \leqslant 42$ in the framework of the Dirac–Fock single-configuration approximation in the late 1980's.[20] Charro *et al.* performed calculations on the M1 and E2 transition probabilities of the 3d $^2D_{3/2}$–3d $^2D_{5/2}$ transition in the K-like sequences with $25 \leqslant Z \leqslant 58$ by using the relativistic quantum defect orbital method.[21] The K-like isoelectronic sequence ions, such as Zn^{11+}, Se^{15+}, have already been produced and studied in the laboratory plasmas.[20] The M1 transition rate of the 3d $^2D_{5/2}$–3d $^2D_{3/2}$ transition in Kr^{17+} has been measured in two experiments using the electron beam ion trap (EBIT).[22,23] This result was not reproducible by an *ab initio* calculation, but combining experimental energies with the calculated transition matrix elements, the results were matching with the measured values within the 1% level.[23] In contrast to K and Ca^+ of the K-like isoelectronic sequence, higher charged ions have the first two low-lying states as 3d $^2D_{3/2,5/2}$ states. This fine-structure splitting becomes larger with increasing in atomic number (Z). Hence, these ions with the forbidden transitions of fine-structure split-

*Project supported by the National Natural Science Foundation of China (Grant Nos. 91436103, 91536102, and 91336211), the Research Programme of National University of Defense Technology, China (Grant No. JC15-0203), and the Strategic Priority Research Programme of the Chinese Academy of Sciences (Grant No. XDB21030300).

†Corresponding author. E-mail: cbli@wipm.ac.cn

‡Corresponding author. E-mail: hxzou@nudt.edu.cn

© 2017 Chinese Physical Society and IOP Publishing Ltd

ting could serve as potential candidates for the HCI clocks. As has been demonstrated in Ref. [9], the monovalent (ns) (np) or divalent $(np)^2$ ions are suitable for clock transitions. The above fine structure splitting with longer lifetime of the upper state can be considered for atomic clocks. The obvious advantages are the low degeneracy and the simplicity of their structures, with respect to other candidates of the nf valence electrons.[6–8,24–28] Following this idea, Yu *et al.* carried out the calculations on various systematics for the 3p $^2P_{1/2}$–3p $^2P_{3/2}$ clock transitions in the Al-like ions with $23 \leqslant Z \leqslant 29$. These transitions were predicted to provide the quality factors $Q \leqslant 3\times10^{14}$.[11] Therefore, it would be desirable to learn whether the K-like ions can be apt for the clock transition in the optical spectral region with higher quality factors.

In this work, we carry out the calculations on the M1 and E2 transition probabilities of the fine-structure splitting of the 3d $^2D_{3/2}$–3d $^2D_{5/2}$ transition along the K-like sequence with $26 \leqslant Z \leqslant 36$ employing the MCDHF method. We analyze contributions from the electron pair correlations and choose an appropriate correlation model for the calculations. Contributions from the Breit and the leading-order QED interactions are also estimated. The lifetimes, linewidth and quality factors are given.

2. Theory and computational details

2.1. MCDHF method

In the MCDHF method, the Dirac-Coulomb Hamiltonian has the form as

$$H_{\rm DC} = \sum_i \left[c\boldsymbol{\alpha}_i\cdot\boldsymbol{p}_i + (\beta_i - 1)c^2 + V_i^N\right] + \sum_{i>j}\frac{1}{r_{ij}}. \quad (1)$$

Here, $\boldsymbol{\alpha}$ and β are the Dirac matrices. V_i^N is the interaction part with the nucleus. The atomic state wave functions (ASFs) are built from the linear combination of the different configuration state wave functions (CSFs) with the same party P, the total angular momentum J and its component along the z direction M_J, which is written as

$$\Psi(\gamma PJM_J) = \sum_{i=1}^{Nc} c_i\Phi(\gamma_i PJM_J). \quad (2)$$

Here, Nc is the number of CSFs, c_i is the mixing coefficient of the corresponding CSF, and γ_i is the additional appropriate labeling to the state i. CSFs are formed by products of one-electron Dirac orbitals; it can be optimized in the self-consistent field (SCF) procedure to minimize the energy eigenvalue as well as the c_i. In the subsequent relativistic configuration interaction (RCI) calculations, only the c_i can be optimized. The Breit interaction in the low-frequency approximation can be taken into account in the procedure, which has the form

$$B_{ij} = -\frac{1}{2r_{ij}}\left[\boldsymbol{\alpha}_i\cdot\boldsymbol{\alpha}_j + \frac{(\boldsymbol{\alpha}_i\cdot\boldsymbol{r}_{ij})(\boldsymbol{\alpha}_i\cdot\boldsymbol{r}_{ij})}{r_{ij}^2}\right]. \quad (3)$$

The leading-order QED effects can be included from the vacuum polarization and self-energy interactions (details can be found in Ref. [29]). All calculations are performed by using the GRASP2K package.[30,31]

2.2. Transition parameters

The transition probabilities A_{ij} between the upper state $\Psi_i(\gamma PJM)$ and the lower state $\Psi_j(\gamma' P'J'M')$ can be expressed as[32]

$$A_{ij} = \frac{2\omega}{c}\frac{1}{(2L+1)(2J+1)}|\langle\Psi_j(\gamma' P'J'M')|\tilde{O}^L|\Psi_i(\gamma PJM\rangle|^2. \quad (4)$$

Here, $\tilde{O}^L$ is an electromagnetic miltipole transition operator of the order L. ω represents the transition frequency. c is the light speed in atomic units. The forms of the E2 transition operators can be expressed as the Coulomb (length) gauge and Babushkin (velocity) gauge.[33] Furthermore, the line strength $S_{ij}^{\rm M1}$ can be defined as

$$S_{ij}^{\rm M1} = \frac{(2J+1)\lambda_{ij}^3}{2.69735\times10^{13}}A_{ij}^{\rm M1}, \quad (5)$$

where λ_{ij} is the transition wavelength in the unit Å. When using the Racah algebra to get the reduced matrix element, it has the assumption that ASFs are built from the same orthonormal radial orbital basis. Since the states of the transitions are always optimized separately to get more accurate results, this constraint is severe. This issue can be overcome by transforming the ASFs of the two states of the transitions into biorthonormal terms.[34]

Furthermore, the lifetime τ_i of the upper state i can be determined by

$$\tau_i = \frac{1}{\sum_{j,{\rm o}}A_{ij}^{\rm o}}, \quad (6)$$

where, the notation "o" represents the transition channels from the state i to the state j,and j represents all the states below the state i.

2.3. Computational model

In order to consider the electron correlations systematically, the active space approach is applied to build the ASFs.[35] According to the perturbation theory, the dominant reference configuration state should be included in the zero-order correlation wavefunction. The set of the first-order ASFs contains all the CSFs obtained by the single and double (SD) substitution of electrons from the occupied orbitals to the virtual orbitals, which can be classified by the substitution of the specific electron pairs.[36] Furthermore, the higher-order set contains the correlations of triple, quadruple or more excitations.

In this work, $\{[{\rm Ne}]3s^23p^63d\}$ is chosen as the reference state for the two concerned 3d $^2D_{3/2,5/2}$ states. To describe

effectively the important correlations in the first step, we calculated the contributions of the individual electron pairs separately in the SCF procedure. The calculations started from Dirac–Hartree–Fock (DHF) approximation, and all occupied orbitals were optimized, but keeping frozen in the subsequent steps. The extended optimal levels (EOL) scheme was applied here. The relaxation effects were eliminated by the simultaneous optimization of the ground and excited states in our calculations.The configurations were generated by the excitations of the specific electron pairs in each step of the active space enlargement. In this manipulation, the contributions of the corresponding pair correlations were obtained.

In order to get the reliable results, contributions of 20 kinds of electron pairs are systematically included, where the active space was taken up to $n = 6$ and $l = 5$. We illustrate the contributions of the different electron-pair correlation in the Zn^{11+} as shown in Fig. 1. In this figure, the y axis shows the kind of electron pair being considered. For example, the label "2s2" represents two electrons in the 2s orbital. The contributions are expressed as the difference between the specific electron pair and the DHF results. One can see that the 2p3d and 3s3p pairs have considerable contributions to the transition properties. Although the 1s2 pair has negligible influence, the pair involving the core shells 1s and 2s can also have an indispensable contribution to the correlation. It is worth noting that the contributions from different electron pairs to the ΔE and A_{M1} have a similar pattern. Similar conclusions were also found in the other ions, which are not shown in this paper.

According to the analysis of correlations of the individual electron pairs, the most important electron correlation effects can be captured. Moreover, to describe efficiently the electron correlations in the orbital basis set, the virtual orbitals are optimized considering the specific electron correlations of these two electron pairs 2p3d and 3s3p. The configuration space is expanded by the substitutions of these two electron pairs from the reference configuration, which means at most one excitation of the electrons is allowed in the 2p, 3d or 3s, 3p orbitals, with no more than two excitations in the corresponding two orbitals. The space is enlarged up to $n = 7$ and $l = 5$, which is labeled as n. The operation of DHF calculation is the same as above and the virtual orbitals are optimized in each new added layer. Subsequently, the other first-order correlations are considered in the RCI procedure. Here, the involving electron correlations of the pairs 2s3s, 1s2p, 2s2p, 2p2, 2s3d, 3p2, 1s3p, 2s3p, 3s2, 3p3d, which have large contributions as shown in Fig. 1, are taken into calculations. The approximation is labeled as nrSD.

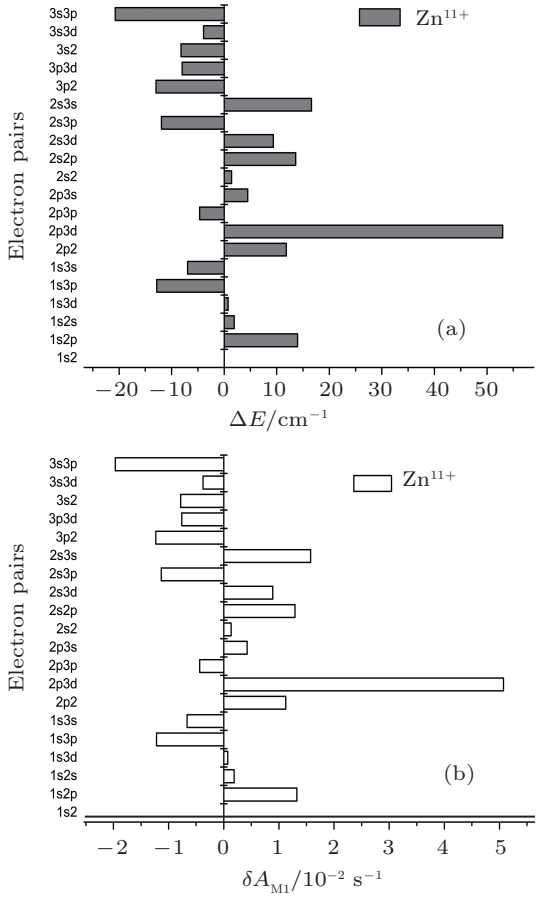


Fig. 1. The contributions of the different electron-pair correlations in Zn^{11+}: (a) to the excitation energy, δE in unit cm^{-1}; (b) to the M1 transition probability, δA_{M1} in unit s^{-1}.

The higher-order correlations were not fully included in the calculations, because the number of CSFs increases rapidly, which is beyond the limitation of the current capacity of our computational facility. Hence, we use the multi-reference (MR) approach to involve the important higher-order correlations into the RCI procedure. In this approach, the dominant configurations $\{[Ne]3s^23p^63d, [Ne]3s^23p^43d^3\}$ in "7rSD" will be selected as the multi-reference set. It should be noted that the latter configuration is degenerate with the former for both the $J = 3/2$ and $J = 5/2$ states in the jj configuration. We performed the results by adding the higher-order correlations to the 7rSD involving the excitations from the important electron pairs 2p3d and 3s3p to the virtual orbitals with $n = 4$. This model is labeled as MR-rSD.

Finally, the Breit interaction and the leading QED effects were considered through RCI computation in the configuration space, which are labeled as "+B" and "+Q", respectively.

3. Results and discussions

In order to verify the validity of the computational model, we show the calculated excitation energy and forbidden transition probabilities of Kr^{17+} as the functions of the computational model in Table 1. Here, $\Delta = |A_{E2}(C) -$

$A_{E2}(B)|/\max(A_{E2}(C),A_{E2}(B))$. Comparing the results obtained from DHF and MR-rSD calculations, ΔE and A_{M1} are not quite sensitive to the electron correlations, leading to changes less than 0.6% and 1.8% on the bases of the DHF results, respectively. Although A_{E2} is smaller than A_{M1} by about 5 orders of magnitude, considerations of the electron correlations make the changes about 17% on it. Comparing the results obtained from the 7rSD and MR-rSD calculations, it can be found that the higher-order correlations cause the relative changes of about 0.07% on the excitation energy, 0.2% on A_{M1}, 0.5% on A_{E2} in the Coulomb gauge and 0.2% on A_{E2} in the Babushkin gauge, respectively. The differences between the DHF/DHF + X, 7rSD/7rSD + X, and MR-rSD/MR-rSD + X (X = B, Q) results show that the contribution of the leading QED effects on the transition properties is as small as about 0.15% on the excitation energy, 0.5% on A_{M1}, 0.4% on $A_{E2}(C)$, and 0.7% on $A_{E2}(B)$, respectively. Contrary to the QED effects, the Breit interaction influences the results considerably on the excitation energy about 6%, 16% on A_{M1}, 31% on $A_{E2}(C)$ and 25% on $A_{E2}(B)$. It is noted that the line strength of M1 transition, S_{M1}, is insensitive to the electron correlations, the Breit interaction and the leading QED effects. It implies that the reliability of A_{M1} can be determined by the accuracy of the calculated ΔE.

Table 1. Excitation energies ΔE in unit cm^{-1}, M1 transition probabilities A_{M1} in unit s^{-1} with the corresponding line strength S_{M1} in unit a.u. and E2 transition probabilities A_{E2} in unit s^{-1} of the $3d\ ^2D_{3/2}$–$3d\ ^2D_{5/2}$ transition for Kr^{17+} as the functions of the computational model. The notations "C" and "B" represent the results of A_{E2} in the Coulomb and Babushkin gauge, respectively. Δ represents the difference between the A_{E2} (B) and A_{E2} (C). The number in square brackets represents the power of 10.

Items	ΔE	A_{M1}	S_{M1}	A_{E2} (C)	A_{E2} (B)	Δ
DHF	16452.8	47.9607	2.3954	3.7079[–4]	3.6708[–4]	9.99[–3]
DHF + Q	16477.4	48.1758	2.3954	3.7245[–4]	3.6983[–4]	7.04[–3]
DHF + B	15527.5	40.3151	2.3954	3.1168[–4]	2.7483[–4]	1.18[–1]
DHF + BQ	15552.1	40.5067	2.3954	3.1316[–4]	2.7701[–4]	1.15[–1]
4	16510.6	48.4677	2.3954	3.3941[–4]	3.0520[–4]	1.01[–1]
5	16514.4	48.5007	2.3954	3.1213[–4]	3.0608[–4]	1.94[–2]
6	16519.6	48.5471	2.3954	3.0244[–4]	3.0603[–4]	1.17[–2]
7	16521.6	48.5638	2.3954	3.0891[–4]	3.0623[–4]	8.66[–3]
7rSD	16539.9	48.7259	2.3954	3.0840[–4]	3.0821[–4]	6.36[–4]
7rSD + Q	16564.6	48.9442	2.3954	3.0968[–4]	3.1047[–4]	2.54[–3]
7rSD + B	15653.9	41.3075	2.3954	2.1407[–4]	2.3425[–4]	8.62[–2]
7rSD + BQ	15678.6	39.7743	2.2956	2.7789[–3]	2.6322[–4]	9.05[–1]
MR-rSD	16550.7	48.8211	2.3954	3.0689[–4]	3.0768[–4]	2.57[–3]
MR-rSD + Q	16575.4	49.0399	2.3954	3.0814[–4]	3.0994[–4]	5.80[–3]
MR-rSD + B	15665.3	41.3981	2.3954	2.1304[–4]	2.3394[–4]	8.93[–2]
MR-rSD + BQ	15690.1	41.5943	2.3954	2.1396[–4]	2.3576[–4]	9.25[–2]
Experiments						
NIST[39]	15695[a]					
Träbert *et al.*[22]		44.1(2.0)				
Guise *et al.*[23]		40.8(5)				
Calculations						
Urrutia *et al.*[40]	15656.8	41.7, 42.0[&]				
Guise *et al.*[23]	15617.0[d]	41.4[b,&], 41.6[c,&]				
		41.02[d], 41.6[d,&]				
Träbert *et al.*[22]		41.89		2.60[–4]		
Charro *et al.*[21]	15969.6	43.9, 41.7[&]		2.21[–4]		
Ali *et al.*[20]	15575.6	40.7, 41.6[&]		2.79[–4]		
Biémont *et al.*[19]	15703.0	41.9, 41.9[&]		2.93[–4]		
Ali *et al.*[37]	15671[e]					

[a] the semiempirical result by Kaufman *et al.*;[38] [b] FAC result; [c] lowest-order RMBPT result; [d] GRASP2K result; [e] the result in the multi-configuration approximation; and [&] the adjusted results presented in Ref. [23].

The calculated excitation energies of Kr^{17+} in Table 1 using 7rSD + BQ and MR-rSD + BQ models differ from the NIST value[39] by about 0.1% and 0.03%. It is implied that, although some of the first-order correlations are neglected, the 7rSD + BQ model can still produce accurate results. The MR-rSD + BQ model can effectively capture the main contributions of the higher-order correlations. As for A_{M1}, our result is in agreement with the recent experimental values by Guise *et al.*[23] at the level of 1%, and almost equals the adjusted values in their work. It is reasonable that the adjusted values of A_{M1} are extrapolated by using the experimental energy values,[38] while our calculated excitation energy has a good agreement with it. In Table 1, the results of other theoretical calculations are listed. Our results on the excitation energy agree with other calculations, with the differences

less than 1%. The transition rates A_{M1} and A_{E2} are also consistent with other calculations.

The results for the excitation energies and the forbidden transition probabilities of the 3d $^2D_{3/2}$–3d $^2D_{5/2}$ transition in the K-like ions with $26 \leqslant Z \leqslant 36$ are presented in Tables 2 and 3. Comparing the results of different computational models, it can be found that, among the contributions to the transition properties, the Breit interaction is the most important one. The influences of the electron correlations to the excitation energies are smaller than the Breit interaction, but it is still significant. The leading-order QED effects are quite small. It is shown that the excitation energies obtained using the MR-rSD + BQ model are in good agreement with the NIST data[39] and the differences are within 0.4%. The relative contribution of QED effects is around 0.15% to the excitation energies. The transition rates A_{M1} and A_{E2} increase rapidly along the sequence, and the M1 transition is the dominant one. It can be said that S_{M1} for all the ions considered in this work are around 2.40 a.u. and they are insensitive to the electron correlations, Breit interaction and the leading QED effects. The electron correlations have more influences on $A_{E2}(C)$ than $A_{E2}(B)$.

Table 2. Excitation energies ΔE in unit cm^{-1} and the M1 transition probabilities A_{M1} in unit s^{-1} of the 3d $^2D_{3/2}$–3d $^2D_{5/2}$ transition for the K-like ions with $26 \leqslant Z \leqslant 36$. For convenience, the notations "D" and "M" are used to represent the models "DHF" and "MR-rSD", respectively. The number in square brackets represents the power of 10.

Items	Fe^{7+}	Co^{8+}	Ni^{9+}	Cu^{10+}	Zn^{11+}	Ga^{12+}	Ge^{13+}	As^{14+}	Se^{15+}	Br^{16+}	Kr^{17+}
ΔE											
D	1975.6	2621.8	3399.3	4324.1	5413.1	6684.0	8155.7	9847.5	11779.9	13974.3	16452.8
D + Q	1978.0	2625.1	3403.7	4329.8	5420.4	6693.3	8167.2	9861.6	11797.0	13994.9	16477.4
D + B	1793.9	2396.1	3123.7	3992.5	5019.0	6220.7	7615.8	9223.5	11063.9	13158.0	15527.5
D + BQ	1796.4	2399.4	3128.1	3998.2	5026.4	6229.9	7627.3	9237.6	11081.0	13178.5	15552.1
M + B	1829.9	2436.9	3171.2	4047.3	5082.1	6293.2	7698.8	9318.2	11171.6	13280.0	15665.3
M + BQ	1832.5	2440.3	3175.7	4053.2	5089.6	6302.5	7710.4	9332.5	11188.9	13300.8	15690.1
NIST[39]	1836	2451	3178	4057	5095	6308	7714	9337[a]	11193[a]	13306[a]	15696
A_{M1}											
D	8.3141[–2]	1.9431[–1]	4.2344[–1]	8.7148[–1]	1.7095	3.2181	5.8452	10.2882	17.6086	29.3915	47.9607
D + Q	8.3449[–2]	1.9505[–1]	4.2509[–1]	8.7495[–1]	1.7164	3.2314	5.8699	10.3324	17.6855	29.5216	48.1758
D + B	6.2249[–2]	1.4832[–1]	3.2858[–1]	6.8599[–1]	1.36276	2.5941	4.7595	8.4537	14.5889	24.5356	40.3151
D + BQ	6.2503[–2]	1.4893[–1]	3.2998[–1]	6.8895[–1]	1.3686	2.6057	4.9391	8.4925	14.6567	24.6510	40.5067
M + B	6.6075[–2]	1.5602[–1]	3.4281[–1]	7.1460[–1]	1.4147	2.6859	4.9168	8.7168	15.0191	25.2246	41.3981
M + BQ	6.6348[–2]	1.5667[–1]	3.4528[–1]	7.1774[–1]	1.4210	2.6979	4.7811	8.7568	15.0888	25.3430	41.5943
Ref. [19]	6.70[–2]	1.60[–1]	3.48[–1]	7.25[–1]	1.43	2.72	4.98	8.83	15.2	25.6	41.9
Ref. [20]	6.67[–2]	1.59[–1]	3.46[–1]	6.95[–1]	1.38	2.62	4.81	8.54	14.7	24.8	40.7
Ref. [21]	9.87[–2]	2.09[–1]	4.25[–1]	8.36[–1]	1.59	2.95	5.32	9.35	16.0	26.8	43.9

[a] Kaufman *et al.*[38]

Table 3. The E2 transition probabilities A_{E2} in unit s^{-1} of the 3d $^2D_{3/2}$–3d $^2D_{5/2}$ transition for the K-like ions with $26 \leqslant Z \leqslant 36$. The same notations "D" and "M" in Table 2 are adopted. Δ_M is the relative difference between $A_{E2}(B)$ and $A_{E2}(C)$ in the model "M + BQ". The number in square brackets represents the power of 10.

Items	Fe^{7+}	Co^{8+}	Ni^{9+}	Cu^{10+}	Zn^{11+}	Ga^{12+}	Ge^{13+}	As^{14+}	Se^{15+}	Br^{16+}	Kr^{17+}
$A_{E2}(C)$											
D	1.1320[–7]	3.2541[–7]	8.6509[–7]	2.1545[–6]	5.0754[–6]	1.1386[–5]	2.4479[–5]	5.0665[–5]	1.0135[–4]	1.9658[–4]	3.7079[-4]
D + Q	1.1362[–7]	3.2665[–7]	8.6846[–7]	2.1631[–6]	5.0961[–6]	1.1433[–5]	2.4583[–5]	5.0883[–5]	1.0179[–4]	1.9745[–4]	3.7245[–4]
D + B	8.4753[–8]	2.4839[–7]	6.7129[–7]	1.6960[–6]	4.0459[–6]	9.1786[–6]	1.9933[–5]	4.1631[–5]	8.3968[–5]	1.6411[–4]	3.1168[–4]
D + BQ	8.5099[–8]	2.4942[–7]	6.7414[–7]	1.7033[–6]	4.0635[–6]	9.2195[–6]	1.2948[–5]	4.1822[–5]	8.4358[–5]	1.6488[–4]	3.1316[–4]
M + B	4.6614[–8]	1.3963[–7]	4.0477[–7]	1.0418[–6]	2.5307[–6]	5.8414[–6]	1.2892[–5]	2.7331[–5]	5.5925[–5]	1.1078[–4]	2.1304[–4]
M + BQ	4.6815[–8]	1.4024[–7]	4.0651[–7]	1.0463[–6]	2.5416[–6]	5.8666[–6]	2.0023[–5]	2.7448[–5]	5.6166[–5]	1.1126[–4]	2.1396[–4]
$A_{E2}(B)$											
D	1.0162[–7]	2.9970[–7]	8.1173[–7]	2.0498[–6]	4.8788[–6]	1.1036[–5]	2.3876[–5]	4.9665[–5]	9.9747[–5]	1.9411[–4]	3.6708[–4]
D + Q	1.0225[–7]	3.0160[–7]	8.1701[–7]	2.0634[–6]	4.9120[–6]	1.1112[–5]	2.4045[–5]	5.0022[–5]	1.00474[–4]	1.9554[–4]	3.6983[–4]
D + B	6.2735[–8]	1.9107[–7]	5.3190[–7]	1.3756[–6]	3.3435[–6]	7.7054[–6]	1.6953[–5]	3.5802[–5]	7.2901[–5]	1.4367[–4]	2.7483[–4]
D + BQ	6.3163[–8]	1.9240[–7]	5.3567[–7]	1.3855[–6]	3.3680[–6]	7.7628[–6]	1.4538[–5]	3.6076[–5]	7.3466[–5]	1.4479[–4]	2.7701[–4]
M + B	5.5923[–8]	1.6728[–7]	4.6089[–7]	1.1830[–6]	2.8609[–6]	6.5718[–6]	1.4431[–5]	3.0446[–5]	6.1983[–5]	1.2219[–4]	2.3394[–4]
M + BQ	5.6304[–8]	1.6844[–7]	4.6414[–7]	1.1914[–6]	2.8817[–6]	6.6201[–6]	1.7081[–5]	3.0676[–5]	6.2455[–5]	1.2313[–4]	2.3576[–4]
Δ_M	1.69[–1]	1.67[–1]	1.24[–1]	1.22[–1]	1.18[–1]	1.14[–1]	1.47[–1]	1.05[–1]	1.01[–1]	9.64[–2]	9.25[–2]
Ref. [19]	7.09[–8]	2.16[–7]	5.84[–7]	1.51[–6]	3.64[–6]	8.34[–6]	1.83[–5]	3.84[–5]	7.80[–5]	1.53[–4]	2.93[–4]
Ref. [20]	7.04[–8]	2.14[–7]	5.80[–7]	1.41[–6]	3.41[–6]	7.85[–6]	1.73[–5]	3.69[–5]	7.41[–5]	1.46[–4]	2.79[–4]
Ref. [21]	7.04[–8]	2.05[–7]	5.34[–7]	1.34[–6]	2.74[–6]	6.74[–6]	1.45[–5]	3.04[–5]	6.05[–5]	1.17[–4]	2.21[–4]

The transition properties for the ions are summarized in Table 4. Here, the linewidth $\Gamma = 1/(2\pi\tau)$, $Q = \nu/\Gamma$, and ν is the transition frequency. Since the contribution of the E2 channel to the total transition rate A is quite small, comparing to the M1 channel, we neglect it in the estimation of the lifetime of the upper states. One can see that A increases rapidly along the Z, so the lifetimes (τ) of the 3d $^2D_{5/2}$ state decrease nearly three orders of magnitude from Fe^{7+} to Kr^{17+}, and the transition linewidths (Γ) increase with the same orders. According to the definition of Q, we calculated the values and found that it decreases slowly along the sequence. The Q values of all ions are larger than 7×10^{13}. For the promising candidates of HCI clocks, it would be better that the clock transition locates in the optical regime with a high Q value. Considering the manipulation process of the atomic clock experiments, the longer lifetime of the upper state of the clock transition is preferable. Although the fine-structure splitting in the ^2D state of Kr^{17+} is 637 nm, which is in the optical region, the lifetime of the 3d $^2D_{5/2}$ state of it is only 24 ms, which is not good enough for the clock experiment. The 3d $^2D_{5/2}$ state of Fe^{7+} has the long lifetime as 15 s and the Q value is also large, but the transition wavelength is 5457 nm, which is not easy to build proper lasers for experiments. As the practical and balanced choice, Cu^{10+} and Zn^{11+} are recommended. The transitions of both ions are in the near infrared region and the lasers could be available. The lifetimes of the 3d $^2D_{5/2}$ state are about 1 s, which is long enough for experiments.

Table 4. The wavelength λ, total transition probabilities A, lifetimes τ, linewidth Γ, and quality factor Q of the 3d $^2D_{3/2}$–3d $^2D_{5/2}$ transition for the K-like ions with $26 \leqslant Z \leqslant 36$. The number in square brackets represents the power of 10.

Items	λ/nm	A/s^{-1}	τ/s	Γ/Hz	Q
Fe^{7+}	5457.15	0.07	15.07	0.0106	5.20[15]
Co^{8+}	4097.91	0.16	6.38	0.0249	2.93[15]
Ni^{9+}	3148.87	0.35	2.90	0.0550	1.73[15]
Cu^{10+}	2467.20	0.72	1.39	0.1142	1.06[15]
Zn^{11+}	1964.79	1.42	0.70	0.2262	6.75[14]
Ga^{12+}	1586.66	2.70	0.37	0.4294	4.40[14]
Ge^{13+}	1296.95	4.78	0.20	0.7861	2.94[14]
As^{14+}	1071.53	8.76	0.11	1.3937	2.00[14]
Se^{15+}	893.74	15.09	0.07	2.4015	1.40[14]
Br^{16+}	751.83	25.34	0.04	4.0335	9.89[13]
Kr^{17+}	637.34	41.59	0.02	6.6199	7.11[13]

4. Conclusion

For the interests of the plasma diagnostic processes and the candidates of the HCI clocks, we have investigated the M1 and E2 transition properties of the fine-structure splitting in ^2D state for the K-like ions for $26 \leqslant Z \leqslant 36$ with the MCDHF method. The results of the excitation energies have good agreements with NIST data and the differences are within 0.4%. The contributions of the electron correlations, Breit interaction, and the leading QED effects are analyzed. It is shown that the good treatment of electron correlations and inclusion of the Breit interaction are essential for the reliable prediction of the transition properties for these ions. In choosing candidates for HCI clocks from the K-like ions in $26 \leqslant Z \leqslant 36$, Cu^{10+} and Zn^{11+} are recommended for the balanced consideration of the Q factor, the lifetime of the clock state and the feasibility of the lasers.

References

[1] Suckewer S and Hinnov E 1978 *Phys. Rev. Lett.* **41** 756
[2] Suckewer S and Hinnov E 1979 *Phys. Rev. A* **20** 578
[3] Lodders K 2003 *Astrophys. J.* **591** 1220
[4] François P, Matteucci F, Cayrel R, Spite M and Chiappini C 2004 *Astron. & Astronphys.* **421** 613
[5] Ovsiannikov V D, Derevianko A and Gibble A 2011 *Phys. Rev. Lett.* **107** 093003
[6] Safronova M S, Dzuba V A, Flambaum V V, Safronova U I, Porsev S G and Kozlov M G 2014 *Phys. Rev. Lett.* **113** 030801
[7] Derevianko A, Dzuba V A and Flambaum V V 2012 *Phys. Rev. Lett.* **109** 180801
[8] Berengut J C, Dzuba V A and Flambaum V V 2010 *Phys. Rev. Lett.* **105** 120801
[9] Yudin V I, Taichenachev A V and Derevianko A 2014 *Phys. Rev. Lett.* **113** 233003
[10] Schmöger L, Versolato O O, Schwarz M, Kohnen M, Windberger A, Piest B, Feuchtenbeiner S, Pedregosa-Gutierrez J, Leopold T, Micke P, Hansen A K, Baumann T M, Drewsen M, Ullrich J, Schmidt P O and López-Urrutia J R C 2015 *Science* **347** 1233
[11] Yu Y M and Sahoo B K 2016 *Phys. Rev. A* **94** 062502
[12] Rynkun P, Jönsson P, Gaigalas G and Fischer C F 2013 *Astron. & Astronphys.* **557** A136
[13] Jönsson P, Radžiūtė L, Gaigalas G, Godefroid M R, Marques J P, Brage T, Fischer C F and Grant I P 2016 *Astron. & Astronphys.* **585** A26
[14] Rynkun P, Jönsson P, Gaigalas G and Fischer C F 2014 *At. Data Nucl. Data Tables* **100** 315
[15] Jönsson P, Alkauskas A and Gaigalas G 2013 *At. Data Nucl. Data Tables* **99** 431
[16] Wang K, Chen Z B, Si R, Jönsson P, Ekman J, Guo X L, Li S, Long F Y, Dang W, Zhao X H, Hutton R, Chen C Y, Yan J and Yang X 2016 *Astro. J. Supp.* **226** 14
[17] Ekman J, Jönsson P, Gustafsson S, Hartman H, Gaigalas G, Godefroid M R and Fischer C F 2014 *Astron. & Astronphys.* **564** A24
[18] Rynkun P, Jönsson P, Gaigalas G and Fischer C F 2012 *At. Data Nucl. Data Tables* **98** 481
[19] Biémont E and Hansen J E 1989 *Phys. Scr.* **39** 308
[20] Ali M A and Kim Y K 1988 *Phys. Rev. A* **38** 3992
[21] Charro E, Curiel Z and Martín I 2002 *Astron. & Astronphys.* **387** 1146
[22] Träbert E, Beiersdorfer P, Brown G V, Chen H, Thorn D B and Biémont E 2001 *Phys. Rev. A* **64** 042511
[23] Guise N D, Tan J N, Brewer S M, Fischer C F and Jönsson P,2014 *Phys. Rev. A* **89** 040502
[24] Nandy D K and Sahoo B K 2016 *Phys. Rev. A* **94** 032504
[25] Dzuba V A, Derevianko A and Flambaum V V 2012 *Phys. Rev. A* **86** 054501
[26] Safronova M S, Dzuba V A, Flambaum V V, Safronova U I, Porsev S G and Kozlov M G 2014 *Phys. Rev. A* **90** 042513
[27] Safronova M S, Dzuba V A, Flambaum V V, Safronova U I, Porsev S G and Kozlov M G 2014 *Phys. Rev. A* **90** 052509
[28] Dzuba V A, Flambaum V V and Katori H 2015 *Phys. Rev. A* **91** 022119
[29] Dyall K G, Grant I P, Johnson C T, Parpia F A and Plummer E P 1989 *Comput. Phys. Commun.* **55** 425
[30] Jönsson P, He X, Fischer C F and Grant I P 2007 *Comput. Phys. Commun.* **177** 597
[31] Jönsson P, Gaigalas G, J. Bieroń, Fischer C F and Grant I P 2013 *Comput. Phys. Commun.* **184** 2197
[32] Grant I P 2007 *Relativistic Quantum Theory of Atoms and Molecules: Theory and Computation* (Springer)
[33] Grant I P, 1974 *J. Phys. B: At. Mol. Opt. Phys.* **7** 1458
[34] Olsen J, Godefroid M R, Jönsson P, Malmqvist P Å and Fischer C F 1995 *Phys. Rev. E* **52** 4499
[35] Fischer C F, Brage T and Jönsson P 1997 *Computational Atomic Structure: An MCHF Approach* (Institute of Physics Publishing, Bristol and Philadelphia)
[36] Zhou F, Qu Y, Li J and Wang J 2015 *Phys. Rev. A* **92** 052505
[37] Ali M A and Kim Y K 1992 *J. Opt. Soc. Am. B* **9** 185
[38] Kaufman V, Sugar J and Rowan W 1989 *J. Opt. Soc. Am. B* **6** 142
[39] Kramida A, Ralchenko Yu., Reader J and NIST ADS TEAM (2016) NIST Atomic Spectra Database (version 5.4) http://physics.nist.gov/asd
[40] López-Urrutia J R C, Beiersdorfer P, Widmann K and Decaux V 1999 *Phys. Scr.* **T80** 448